Flux jumps in hot-isostatic-pressed bulk MgB_2 superconductors: Experiment and theory

C. Romero-Salazar,* F. Morales, and R. Escudero†
Instituto de Investigaciones en Materiales, Universidad Nacional Autónoma de México, Apartado Postal 70-360, México, Distrito Federal 04520, Mexico

A. Durán
Centro de Ciencias de la Materia Condensada, Universidad Nacional Autónoma de México, Apartado Postal 2681, Ensenada, Baja California 22800, Mexico

O. A. Hernández-Flores
Instituto de Física, Universidad Autónoma de Puebla, Apartado Postal J-48, Puebla, Puebla 72570, Mexico
(Received 28 May 2007; published 27 September 2007)

An experimental and theoretical study of flux jumps in magnetization curves of a highly dense polycrystalline MgB_2 superconductor was performed. The local temperature increments in the vortex phase were modeled. For the theoretical analysis, a critical-state model was employed which considers Joule's heat dissipation due to temporal evolution of the magnetic induction. We used an adiabatic approximation to define an instability criterion on the shielding field with the Maxwell equations coupled to the thermal diffusion equation. Comparing experimental and theoretical magnetization loops, we found that the flux jump occurrence depends on the flux jump size.

DOI: 10.1103/PhysRevB.76.104521 PACS number(s): 74.70.Ad, 74.25.Ha, 74.25.Sv, 74.81.Bd

I. INTRODUCTION

The discovery of superconductivity at 39 K in the simple binary compound MgB_2 (Ref. 1) has generated numerous experimental and theoretical studies in order to understand its electronic properties. From the technical point of view, many efforts have been made to find optimal characteristics of this compound in order to produce high critical current densities, J_c, and consequently generate intense magnetic fields.

Research on samples prepared on different forms[2,3] has shown that the superconducting currents in the MgB_2 material do not exhibit weak-link effects as in the high T_c superconductors. However, an effect noted in type-II superconductors, with low heat capacity and possibility to transport high J_c, has been the presence of flux avalanches and a complex vortex behavior. Indeed, local temperature increments may produce flux jumps, which is a negative process for practical applications.

Magnetothermal instabilities, such as the flux jumps in magnetization curves[3–17] or dendritic vortex avalanches, directly observed in thin films,[15,18–22] are dramatic features that can occur in type-II superconductors above the first critical field. It is well established that the critical state of a type-II superconductor is unstable since it can be affected by small temperature fluctuations or by variations of the external magnetic field. Flux jumps, which are thermally triggered, tend to destroy the critical state.

The motion of flux lines produces a temporal change of the magnetic induction and an electric field E appears, according to the induction law $\nabla \times \mathbf{E} = -\dot{\mathbf{B}}$. Thus, energy per unit volume is dissipated at a rate $\dot{Q} = \mathbf{E} \cdot \mathbf{J}$. In the meantime, a local increment of the temperature causes J_c to decrease. Experimental observations have demonstrated that flux jumps can only occur if $\partial J_c / \partial t < 0$. As J_c decreases, the magnetic flux penetrates the sample deeply and more heat is released. Eventually, this feedback process causes a dynamics of vortex avalanche type on a large region of the sample,[20,23] decreasing the magnetization.

Recently, Chabanenko *et al.*[4] observed flux jumps in hysteresis loop measurements on a polycrystalline MgB_2 sample. They suggested the applicability of the so-called adiabatic approximation, performing an estimation of the thermal and magnetic diffusion coefficients. Additionally, they estimated the temperature at the sample after a flux jump in a range of external fields H_a less than the penetration field $\mu_0 H_p$.

The vortex avalanche process depends on the relation between thermal and magnetic diffusivities. As pointed out by Chabanenko *et al.*, the magnetic diffusivity is much larger than the thermal diffusivity[4,24] in MgB_2 samples.

In thin films with thickness $d \leqslant \lambda$, where λ represents the London penetration depth, avalanches have been observed in magneto-optical-imaging (MOI) experiments. The magnetic flux penetration occurs abruptly as dendrite flux patterns, instead of the well-known homogeneous Bean's magnetic profiles.[15,18–22] It is necessary to emphasize that the powerful MOI technique measures profiles of the perpendicular flux density component, B_z. It is restricted to the study of vortex dynamics in thin films or strips, because one can use the sheet current approximation to reconstruct the magnetic flux distribution $\mathbf{B}(\mathbf{r})$.[25] However, for bulk samples or rectangular plates, with thickness $d > \lambda$, the sheet current approximation is not valid, and hence the entire $\mathbf{B}(\mathbf{r})$ cannot be reconstructed from magneto-optic measurements. On the other hand, the micro-Hall sensors detect vortex avalanches under the Hall area,[4,24] but it has no spatial and temporal resolution of the MOI technique.

Conventional Bean's critical-state model[26] has been very successful in reproducing static magnetization curves, hys-

teresis losses, current transport, and flux trapping of irreversible type-II superconductors in the critical state. However, it cannot model any field instability, and consequently, cannot reproduce magnetothermal instabilities and flux avalanches. To analyze and explain these phenomena, Swartz and Bean[5] presented their adiabatic critical-state scheme, including heating effects. They proposed an instability condition to calculate qualitatively the magnetic field when the first flux jump occurs. In addition, Mints and Rakhmanov[23] performed an extensive study of the critical-state stability and its relation with the flux jump phenomenon. Afterward, Müller and Andrikidis[8] employed the simplest Bean model, with $J=J_c\,\mathrm{sign}(E)$. They analytically calculated magnetization curves for melt-textured $YBa_2Cu_3O_{7-d}$ samples. More recently, Zhou and Yang[16] reported theoretical calculations of flux jumps, employing parameters corresponding to $Bi_2Sr_2CaCu_2O_{8+d}$ samples. They considered the particular case when all the flux jumps have the same size and are complete; thus, the magnetization decreases to zero at each jump.

This work is concerned with both theoretical and experimental studies on the vortex dynamics and flux jumps in hot-isostatic-pressed (HIP) high-quality MgB_2 bulk samples. Experimentally, we performed isothermal measurements of the magnetization versus magnetic field ($\langle M\rangle$ vs H_a) at different temperatures, from 2 up to 25 K. Temperature and magnetic field ranges where the flux jumps appeared were determined. We observed a complex behavior at the lower measured temperatures. The number of events decreases as the temperature increases. At high temperatures, isothermal magnetization measurements show a notable decrease of the number of flux jumps. In order to study the nonisothermal flux distribution in type-II superconductors, we also performed theoretical calculations related to the electromagnetic properties when flux jumps are triggered by local temperature increments. The theoretical model uses an adiabatic critical-state model which considers both the magnetic field and temperature dependence of the critical current density $J_c(B,T)$. The current-carrying ability, the local heating, the instability process that originates the flux jumps, and the flux redistribution toward a metastable critical state after flux jumps occur are modeled. Our theoretical hysteresis curves agree quite well with the corresponding experimental curves in the whole range of temperature studied. We found that the flux jump occurrence depends on the flux jump size.

II. THEORY

To study the magnetic behavior of the bulk MgB_2 HIP samples in critical state under the presence of an external magnetic field $\mathbf{H}_a$ parallel to the sample surface, we consider the following.

(1) The critical-state problem is studied in the framework of a macroscopic approach, in which all lengths are larger than the flux-line spacing; thus, the superconductor is considered as a uniform medium.

(2) Since we consider the Bean isotropic critical state, the current density $\mathbf{J}$ and the electric field $\mathbf{E}$ are parallel [Eq. (3)].

(3) The MgB_2 superconductor is determined by its pinning characteristics; therefore, there is no macroscopic geometric barrier in the magnetization measurements.[27]

(4) It is assumed that the magnetic induction obeys the linear (material) equation $\mathbf{B}=\mu_0\mathbf{H}$. This is an excellent approximation when $B \gg \mu_0 H_{c1}$. The bulk MgB_2 sample satisfies this condition.

(5) In such a parallel geometry, demagnetization effects are not crucial as in the case of an external magnetic field perpendicular to the sample surface.

A. Quasistationary magnetic induction $B(x)$ distributions

The model considers an irreversible, isotropic, type-II superconducting plate (infinite) with thickness d, subject to a varying magnetic field $\mathbf{H}_a=H_a\hat{z}$, parallel to the sample surface.

To describe the magnetic response of the sample, in the Bean critical state,[26] Maxwell's equations are used,

$$\frac{\partial B_z}{\partial x} = -\mu_0 J_y, \tag{1}$$

$$\frac{\partial E_y}{\partial x} = -\frac{\partial B_z}{\partial t}. \tag{2}$$

Since we consider quasistationary states, electric fields in the superconductor are extremely small and the time derivative of the electric displacement can be completely disregarded. To close the system of equations (1) and (2), the following voltage-current relation is used:

$$\mathbf{E} = E(J)\frac{\mathbf{J}}{J}, \tag{3}$$

where

$$E(J) = \begin{cases} 0, & J \leqslant J_c(B,T) \\ \rho[J - J_c(B,T)], & J \geqslant J_c(B,T). \end{cases} \tag{4}$$

Here, $J_c(B,T)$ is the critical value of the current density $\mathbf{J}$ and is a parameter given by the condition of balance between pinning and Lorentz forces acting on the vortices. The resistivity ρ plays the role of an auxiliary parameter.

The magnetic induction depends only on x and on the boundary conditions $\mathbf{B}(x=0)=\mathbf{B}(x=d)=\mu_0\mathbf{H}_a$.

The system of equations (1)–(3) can be solved only numerically. We obtain quasistationary magnetic induction profiles $\mathbf{B}(\mathbf{x})$ for a given external magnetic field $\mathbf{H}_a$. The numerical method employed here is similar to that used by Romero-Salazar and Pérez-Rodríguez.[28]

We are interested in the stability of the critical state related to the effect of the flux and temperature redistribution dynamics. Thus, to compute the heat released due to flux motion, one has to solve the system of equations (1)–(3) plus the heat diffusion equation (6). Indeed, to determine Joule's heat $J_c(B,T)E$, the electric field distribution should be calculated from Faraday's induction law:

$$E = -\int_{d/2}^{x} \frac{\partial B}{\partial t} dx, \quad x > d/2, \tag{5}$$

where the limits of integration have been established using the fact that $E(-J) = -E(J)$.[29]

It is necessary to emphasize that a calculation of the electric field, directly from the material law [Eq. (3)], is not correct because such a relation can recreate approximately the critical environment. Thus, if one considers that the voltage-current relation [Eq. (3)] corresponds to the electric field equation, relevant information may be lost.[30] Moreover, when magnetization measurements are performed, it is well established that the electric field is determined by temporal evolution of the magnetic induction.

B. Instability criterion to find flux jump occurrence

An important step of this model is the use of the adiabatic approximation[5] to approach the critical-state instability and the flux jump problem. One considers that as the applied field $\mathbf{H}_a$ is increased by a small amount ΔH_a ($|\Delta H_a| \ll |H_a|$), through infinitesimal increments δH_a ($|\delta H_a| \ll |\Delta H_a|$), the magnetic flux lines start to penetrate the sample. The magnetic field distribution $B(x)$ is calculated at each step δH_a.

Flux jumps and, consequently, the magnetic field and current density distributions depend on the competition between diffusive and dissipative processes. Because the magnetic flux diffusion is faster than the heat flux, the heating of the superconducting sample is adiabatic. Additionally, it is considered that the sample is not in thermal contact with any surface. Therefore, neglecting the diffusive term in the heat equation, one yields

$$C\frac{dT}{dt} = J_c(B,T)E, \tag{6}$$

where C is the specific heat of the superconducting material. If the temperature is increased locally, the current density is reduced by the amount ΔJ_c and a new profile is established. We used the assumption that the critical current density $J_c(B,T)$ has a linear dependence on the temperature.[5,14] The B-field dependence of the function $J_c(B,T)$ is similar to that used by Cave and LeBlanc[31] and Pérez-González and Clem;[32] thus,

$$J_c(B,T) = J_c(0,T)\left(1 - \frac{B}{B^*}\right)^n, \quad n > 1, \tag{7}$$

with

$$J_c(0,T) = -\left[\left(1 - \frac{B_p}{B^*}\right)^{1-n} - 1\right]\frac{2B^*}{(1-n)\mu_0 d} \times \left[\left(1 - \frac{T}{T_c}\right) \Big/ \left(1 - \frac{T_B}{T_c}\right)\right]. \tag{8}$$

Here, T is the local average temperature reached by the sample, after flux lines penetrate, T_B is the bath temperature where the magnetization measurements are performed, T_c is the superconducting transition temperature, B_p is the penetration field, $B^* = \mu_0 H^*$ is a constant field that characterizes the degree of B dependence of the critical current density $J_c(B,T)$, d is the thickness of the sample, and n is the decay-law exponent of the critical current density.

The reduction of $J_c(B,T)$ decreases the shielding ability of the superconductor by a factor ΔH_{sh}. Such a shielding field decrement is given by

$$\Delta H_{sh} = -\mu_0 \int_0^d \Delta J_c \, dx. \tag{9}$$

Therefore, if $\Delta H_{sh} > \Delta H_a$, the magnetic field configuration becomes unstable and a flux jump takes place. Equation (9) is the so-called *instability criterion*. In other words, if a flux jump occurs, the temperature in the sample increases and a new magnetic field (corresponding to a new critical current density) is established. After the flux jump occurs, the temperature drops back to the bath temperature T_B but the magnetic field profile stays.

C. Flux jump size and magnetization

It is necessary to note that the critical-state models study only quasistationary states; thus, *during* a flux jump, the magnetization cannot be determined since the sample is in a highly nonequilibrium state. Additionally, as far as we know, it is not possible to predict theoretically the size of a flux jump. Indeed, the instability criterion [Eq. (9)] provides the magnetic field value where a flux jump occurs, but does not contain any information about the size of such an event. However, it is well established that the critical current density is reduced due to a flux jump. Therefore, in the numerical procedure, it is not possible to calculate how much the critical current density diminishes; here, we define the size of a flux jump as the ratio α proposed earlier by Chabanenko *et al.*:[14]

$$\alpha = \frac{\text{critical current density after the flux jump}}{\text{critical current density before the flux jump}}. \tag{10}$$

This ratio relates the critical current density values after and before the flux jump. If the instability criterion [Eq. (9)] is satisfied, the critical current density is reduced using α [Eq. (10)] and new values of the magnetic induction distribution and magnetization are calculated. For the corresponding magnetic field profile with or without a flux jump, the average magnetization of the superconducting sample is calculated as

$$\langle M \rangle = \frac{1}{d}\int_0^d \left(\frac{B(x)}{\mu_0} - H_a\right) dx. \tag{11}$$

Afterward, the theoretical magnetization curve is compared with the experimental one. If there is a good fit, the hysteresis calculation $\langle M \rangle$ vs H_a is continued; otherwise, another α value is selected. This procedure allows us to reproduce both partial and complete flux jumps. The main result of this paper lies in the method presented in this section which, as we will show, reproduces isothermal experimental magnetization $\langle M \rangle$ vs H_a loops.

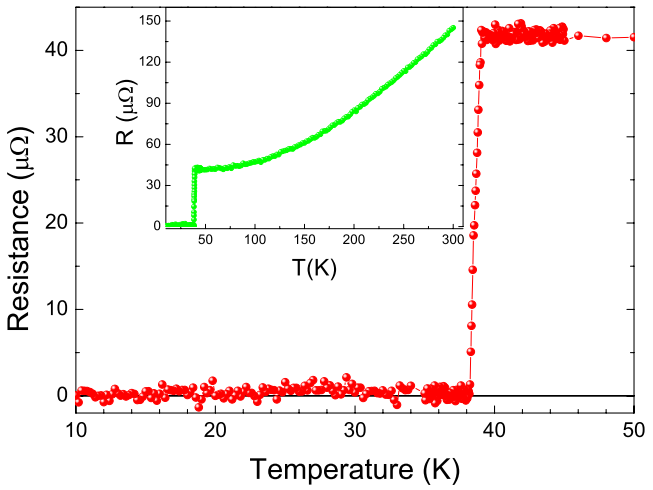

FIG. 1. (Color online) Resistance as a function of temperature around the resistive transition temperature T_c=38.6 K for the HIP MgB_2 sample in zero magnetic field. The width of the transition taken from the onset to R=0 was about ΔT=1 K. The resistance ratio from room temperature to 40 K is equal to 3.52.

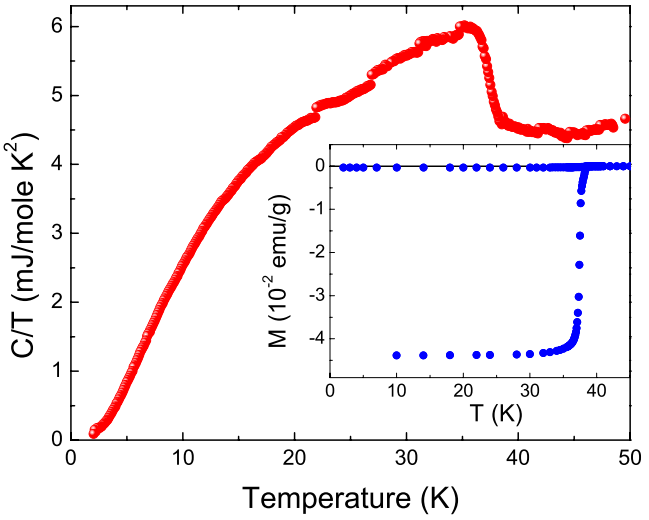

FIG. 2. (Color online) Specific heat divided by temperature C/T vs T at zero external applied field of the HIP MgB_2 sample. Inset: dc magnetization vs temperature curve in a magnetic field of 20 Oe measured at ZFC and FC modes.

III. EXPERIMENT

The polycrystalline MgB_2 sample was sintered starting from MgB_2 powders of −325 mesh size with 98% purity obtained from Alfa Aesar, Inc. In order to compact the sample, the powder was HIP at 200 MPa, employing a dense material cooling under pressure process. Technical details about the sample preparation can be found in Ref. 33. Magnetization, specific heat, and transport measurements were performed in a sample with m=6.73 mg. The density ρ =2.666 g/cm^3 used in this paper was also given in Ref. 33.

For the magnetic measurements, we used a superconducting quantum interference device magnetometer (Quantum Design). dc magnetic susceptibility M and magnetization cycles $\langle M \rangle$ up to ±4 T were performed. The hysteresis loops were obtained in the zero-field-cooling (ZFC) mode at temperatures of 2, 5, 7, 10, 15, 20, 23.5, and 25 K. The surface sample orientation was approximately parallel to the external magnetic field. Determination of the superconducting transition temperature was performed at 20 Oe in ZFC and field-cooling (FC) modes. In the FC mode, the sample presents a normal diamagnetic Meissner effect, different from the paramagnetic effect found by Felner *et al.*[17] The resistance measurements were obtained by the four probe method using a Quantum Design physical property measurement system (PPMS). The resistive transition temperature at half points of the 10%–90% was determined to be T_c=38.6 K. The width of the transition taken from the onset to R=0 was about ΔT=1 K and the resistance ratio was equal to 3.52. These data are depicted in Fig. 1. The superconducting transition temperature, determined by magnetization measurements at 20 Oe, was T_c=38.5 K. The curve is depicted in the inset of Fig. 2. Data are presented in the temperature range of 2–50 K. Specific heat C measurements were performed at zero external magnetic field, from room temperature down to 2 K, in the PPMS system. Figure 2 shows the specific heat divided by temperature C/T vs T curve. The specific heat has small values, characteristic of this kind of samples, which also presents an anomalous behavior as was found by Frederick *et al.*[33]

IV. NUMERICAL RESULTS AND COMPARISON WITH EXPERIMENT

As was mentioned in Sec. II, we have considered an isotropic superconducting plate (bulk sample) in an external field H_a parallel to its surface.

In order to compare theoretical and experimental measurements, we considered that the applied magnetic fields obey the inequality $\mu_0 H_a \geqslant \mu_0 H_{c1} \sim 28-48$ mT.[2] The model sample has a thickness d=1.35 mm, same as the experimental one.

Figures 3 and 4 exhibit our experimental results (left curves) for the magnetization cycles of the highly dense MgB_2 sample measured at eight temperatures: 2, 5, 7, 10, 15, 20, 23.5, and 25 K. The arrows in the top experimental curves of Figs. 3 and 4 show the direction of the increasing and/or decreasing magnetic field. The corresponding theoretical results are presented at the right side of each figure. We observed at the lowest temperature, 2 K, a high number of flux jumps; some of them depressed the magnetization up to zero value. As the bath temperature is increased, the number of flux jumps decreases. From 15 to above 20 K, only one or two jumps are observed. Above 25 K, the curve $\langle M \rangle$ vs H_a presents a behavior without flux jumps. We want to emphasize about the shape of the experimental isothermal magnetization plots: It seems that in the first and third quadrants, where the magnetic field magnitude increases, the number of flux jump events is higher than in the other two quadrants where the magnetic field decreases. Also, it is noted that the stability of the second and fourth quadrants is better than that of the first and third quadrants. We mean by stability a small

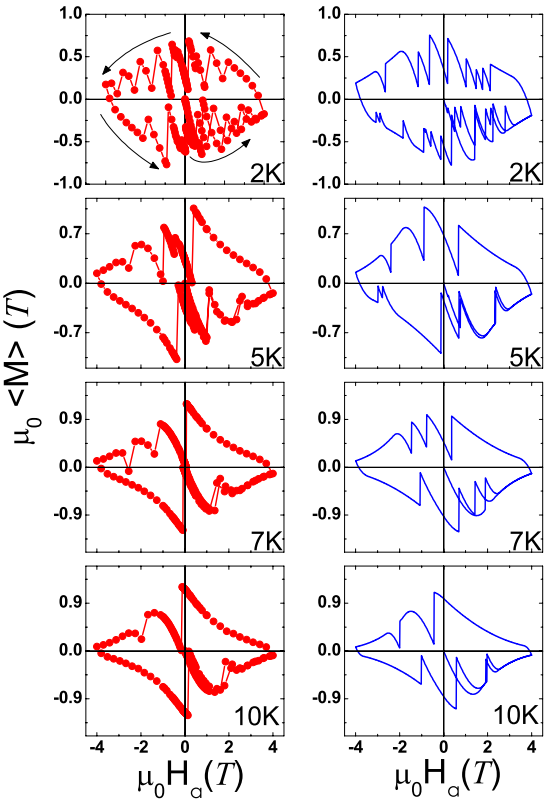

FIG. 3. (Color online) Experimental (left) and theoretical (right) magnetization hysteresis loop data, for applied magnetic fields up to 4 T, measured at four different bath temperatures, T_B=2, 5, 7, and 10 K. The top experimental curve shows the direction of the increase and/or decrease of the applied magnetic field.

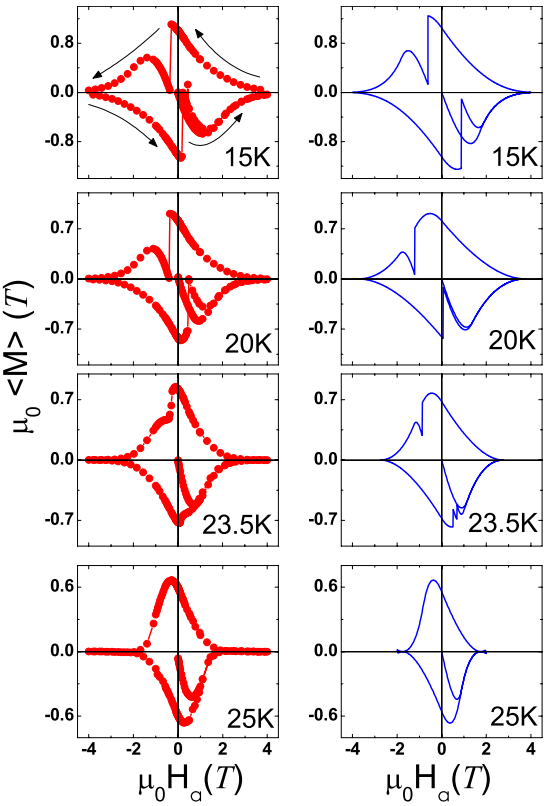

FIG. 4. (Color online) Experimental (left) and theoretical (right) magnetization hysteresis loop data, for applied magnetic fields up to 4 T, measured at four different bath temperatures, T_B=15, 20, 23.5, and 25 K. The top experimental curve shows the direction of the increase and/or decrease of the applied magnetic field.

number of jump events at any temperature. In addition, the hysteresis curves seem to show replicas between the first and third quadrants and between the second and fourth quadrants. This general behavior was also seen by other researches in measurements performed with high temperature superconducting materials, although at different temperature ranges.[4,8,17]

The magnetic process in superconducting materials occurs in the following manner: The flux vortex in the sample starts at the surface and is displaced to the interior of the sample, until the equilibrium between the gradients of Lorentz force and the pinning forces is obtained. Once the pinning force is less than the magnetic force, one vortex avalanche is produced with the consequent release of Joule heat. At this moment, the temperature will rise, inclusive above T_C, and in consequence, the magnetization decays to zero. The field at which the avalanche occurs is the field necessary to produce the Lorentz force that breaks the pinning. When the sample recovers to the bath temperature, the field profile may be different. At this point, the competing process between the Lorentz and pinning forces starts again; meanwhile, the applied field is increased. It was sometimes assumed that this avalanche process may occur periodically with respect to the field; however, this effect was not observed experimentally, probably due to different internal and external effects, such as the different field profiles, thermal and magnetic fluctuations, influence of metallic impurities, and trapped field inside of the material. For the case when the magnetic field is decreasing, as occurs in the second and the fourth quadrants, we must remember that the magnetic field inside the sample is higher than the external magnetic field due to the trapped field; then, the process to expel the field requires less energy than the process to push the field inside of the sample. Thus, when the field is decreased, the process is more stable, and therefore a lower number of flux jumps will be created, as readily observed. It is important to mention that a quantitative physical explanation for the flux jump behavior still requires more study.

Table I presents the main parameters determined from experimental data and from theoretical calculation. The first column is the bath temperature T_B for each hysteresis curve measurement. Specific heat C data at eight different bath temperatures are extracted from the curve of Fig. 2, C/T vs T, measured at zero external magnetic field. It is well established that the specific heat C values depend on the external magnetic field. However, for our numerical calculations, we employed the C values presented in Table I. The penetration field B_p values were obtained from direct inspection of the experimental magnetization curves. In the numerical calculations, B^* is a fit parameter determined when there is a good accordance between experimental and theoretical curves. Equation (7) establishes that when the variable B reaches the

TABLE I. Parameters of the MgB_2 determined from the experimental measurements and from the theoretical calculation. Specific heat C was determined using the experimental data. The critical current density J_c was calculated using the empirical function [Eq. (7)]. n is the coefficient of the decay law of J_c. T_B, B_p, and B^* are the bath temperature, penetration field, and a phenomenological parameter, respectively.

T_B (K)	C (J/K m^3)	B_p (T)	B^* (T)	n	$J_c(B=0,T)$ (10^9 A/m^2)
2	20	1.5	7	2	2.25
5	430	1.82	6.7	2.5	3.20
7	1140	1.9	6.8	3	3.71
10	2830	1.7	7	3.5	3.32
15	7400	1.7	4.5	3	4.20
20	14 180	1.2	3.75	1.75	1.98
23.5	20 640	1.15	2.75	2	2.33
25	23 850	0.9	1.75	2	2.18

B^* value, the critical current density is null, and consequently, the magnetization decreases to zero at this field value. The B^* values are in the range between 1.75 and 7 T. At each temperature of the thermal bath, it was necessary to choose a corresponding B^* value in order that the $\langle M\rangle$ vs H_a curve fits the experimental one. The decay-law exponent of the critical current density, parameter n, was determined for a good fitting with each experimental hysteresis cycle. Finally, the theoretical maximum value of the critical current density, $J_c(0,T)$, corresponding to each of the eight temperatures is presented in the last column of the table. The order of magnitude of the theoretical $J_c(0,T)$ is in good agreement with other values previously reported.[4]

With all the above information, we were able to numerically calculate the theoretical hysteresis loops. For all bath temperatures, it is worth noting the excellent agreement between experimental and theoretical values, including the occurrence of the partial and complete flux jumps. However, we must observe that at low bath temperatures, 2, 5, 7, and 10 K (see Fig. 3), there exists an extra persistent flux jump in the theoretical curves at the fourth quadrant in comparison to the experimental ones. This causes further flux jumps to be shifted to the first quadrant. Finally, in our approach, we select an α value for each of the four quadrants of the hysteresis curve.

We emphasize that the flux jump occurrence depends on the flux jump size α. Let us describe this fact using Fig. 5. The three magnetization curves correspond to the same temperature bath at $T=5$ K. They were created in a range of applied external fields $\mu_0 H_a$ from 0 to 4 T. The only difference lies in the flux jump size α. The solid line corresponds to $\alpha=0$, the dashed line to $\alpha=0.01$, and the dot dashed line to $\alpha=0.025$. Even though the first instability at $\mu_0 H_a \sim 1$ T can be reproduced for each of the three α values, the later events are highly sensitive to α. For $\alpha=0$, the critical current density goes to zero at $\mu_0 H_a \sim 1$ T; thus, the magnetization is also zero at this external magnetic field and the flux jump is complete. However, for this α, there is not a second event.

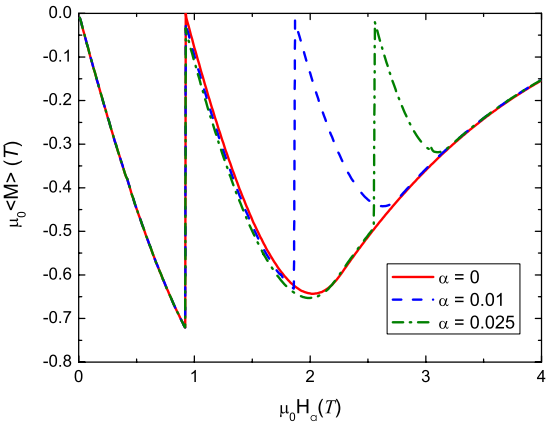

FIG. 5. (Color online) Theoretical magnetization curves, $\mu_0\langle \mathbf{M}\rangle$, for an external magnetic field $\mu_0 H_a$ that varies from 0 to 4 T for a MgB_2 model sample at $T_B=5$ K. Compare with the corresponding experimental and theoretical hysteresis in Fig. 3. Here, we presented three curves where the first flux jump, which always occurs at the same $\mu_0 H_a \sim 1$ T, has a different size. One can observe how the size of the first flux jump determines the occurrence of further events. See text for details.

On the other hand, for $\alpha=0.01$, a second flux jump appears but at an external magnetic field $\mu_0 H_a \sim 2$ T, which is less than the experimental one. This fact is clear if one compares such a theoretical curve with the corresponding experimental curve at $T=5$ K in Fig. 3. Only for $\alpha=0.025$ does the second flux jump arrive at $\mu_0 H_a \sim 2.5$ T, as the experimental one.

This complex behavior differs from the results obtained by Müller and Andrikidis.[8] Indeed, they used the commonly used Bean-type expression to estimate the instability field values. Those values were chosen to fit with their experimental data. In our theoretical calculations, we used a modified Kim-type critical current density, with a linear dependence on the temperature [see Eq. (7)]. Moreover, to analyze if an instability occurs, we used the complex and more general equation, Eq. (9), at each variation of the external field H_a. Recently, Zhou and Yang[16] calculated numerical hysteresis loops. However, they solved the particular case when all the flux jumps depressed completely the magnetization.

Lastly, it is important to mention that the flux jump size calculation is rather complex, being yet an open problem.

V. CONCLUSIONS

We have performed an experimental and theoretical study of the magnetothermal instabilities' effects in the type-II superconductor MgB_2. The flux jumps in the magnetization loops of a HIP high-quality MgB_2 bulk sample were theoretically reproduced using a numerical scheme based on an adiabatic critical-state model. The heat diffusion equation, coupled with Maxwell's equations and material law, was numerically solved. For this purpose, the electric field was calculated from the temporal evolution of the magnetic induction distributions. Our model reproduced all features of the experimental data. We modeled the effect of the flux jumps on the magnetization curves with a parameter α defined as

the ratio of the critical current densities after and before such an event. It was found that the flux jump occurrence depends on this ratio.

ACKNOWLEDGMENTS

We thank M. B. Maple of UCSD and D. H. Galvan of the CCMC-UNAM for kindly providing the MgB_2 sample. C.R.-S. thanks F. Pérez-Rodríguez for helpful discussions and acknowledges support by CONACYT under Grant No. SEP-2004-C01-46425. R.E. acknowledges support of DGAPA-UNAM. We also thank F. Silvar for helium provisions.

*Present address: Institut für Materialphsik, Friedrich Hund Platz 1, 37077 Göttingen, Germany.

†Author to whom correspondence should be addressed; escu@servidor.unam.mx

[1] Jun Nagamatsu, Norimasa Nakagawa, Takahiro Muranaka, Yuji Zenitani, and Jun Akimitsu, Nature (London) **410**, 63 (2001).

[2] C. Buzea and T. Yamashita, Supercond. Sci. Technol. **14**, R115 (2001).

[3] A. Gümbel, J. Eckert, G. Fuchs, K. Nenkov, K.-H. Müller, and L. Schultz, Appl. Phys. Lett. **80**, 2725 (2002).

[4] Victor Chabanenko, Roman Puźniak, Adam Nabialek, Sergei Vasiliev, Vladimir Rusakov, Loh Huanqian, Ritta Szymczak, Henryk Szymczak, Jan Jun, Janusz Karpiński, and Vitaly Finkel, J. Low Temp. Phys. **130**, 175 (2003).

[5] P. S. Swartz and C. P. Bean, J. Appl. Phys. **39**, 4991 (1968).

[6] Y. B. Kim, C. F. Hempstead, and A. R. Strnad, Phys. Rev. **129**, 528 (1963).

[7] L. J. Neuringer and Y. Shapira, Phys. Rev. **148**, 231 (1966).

[8] K.-H. Müller and C. Andrikidis, Phys. Rev. B **49**, 1294 (1994).

[9] S. X. Dou, X. L. Wang, J. Horvat, D. Milliken, A. H. Li, K. Konstantinov, E. W. Collings, M. D. Sumption, and H. K. Liu, Physica C **361**, 79 (2001).

[10] T. C. Shields, K. Kawano, D. Holdom, and J. S. Abell, Supercond. Sci. Technol. **15**, 202 (2002).

[11] Kunitoshi Murai, Jun'ya Hori, Yoshiko Fujii, Johan Shaver, and Gregory Kozlowski, Cryogenics **45**, 415 (2005).

[12] H. P. Goeckner, H. Claus, and J. S. Kouvel, Physica C **418**, 93 (2005).

[13] Seung Hwan Shim, Kwang Bo Shim, and Jong-Won Yoon, J. Am. Ceram. Soc. **88**, 858 (2005).

[14] V. V. Chabanenko, A. I. D'yachenko, A. V. Chabanenko, M. V. Zalutsky, H. Szymczak, S. Piechota, and A. Nabialek, Supercond. Sci. Technol. **11**, 1181 (1998); V. V. Chabanenko, A. I. D'yachenko, A. V. Chabanenko, H. Szymczak, S. Piechota, A. Nabialek, and N. D. Dung, J. Appl. Phys. **83**, 7324 (1998); V. V. Chabanenko, A. I. D'yachenko, M. V. Zalutskii, V. F. Rusakov, H. Szymczak, S. Piechota, and A. Nabialek, *ibid.* **88**, 5875 (2000).

[15] S. C. Wimbush, B. Holzapfel, and Ch. Jooss, J. Appl. Phys. **96**, 3589 (2004).

[16] You-He Zhou and Xiaobin Yang, Phys. Rev. B **74**, 054507 (2006).

[17] I. Felner, V. P. S. Awana, Monika Mudgel, and H. Kishan, J. Appl. Phys. **101**, 09G101 (2007).

[18] T. H. Johansen, M. Baziljevich, D. V. Shantsev, P. E. Goa, Y. M. Galperin, W. N. Kang, H. J. Kim, E. M. Choi, M.-S. Kim, and S. I. Lee, Europhys. Lett. **59**, 599 (2002).

[19] A. V. Silhanek, S. Raedts, and V. V. Moshchalkov, Phys. Rev. B **70**, 144504 (2004).

[20] E. Altshuler and T. H. Johansen, Rev. Mod. Phys. **76**, 471 (2004).

[21] Ruslan Prozorov, Daniel V. Shantsev, and Roman G. Mints, Phys. Rev. B **74**, 220511(R) (2006).

[22] J. Albrecht, A. T. Matveev, J. Strempfer, H.-U. Habermeier, D. V. Shantsev, Y. M. Galperin, and T. H. Johansen, Phys. Rev. Lett. **98**, 117001 (2007).

[23] R. G. Mints and L. Rakhmanov, Rev. Mod. Phys. **53**, 551 (1981).

[24] E. Altshuler, T. H. Johansen, Y. Paltiel, Peng Jin, K. E. Bassler, O. Ramos, Q. Y. Chen, G. F. Reiter, E. Zeldov, and C. W. Chu, Phys. Rev. B **70**, 140505(R) (2004).

[25] Ch. Jooss, J. Albrecht, H. Kuhn, S. Leonhardt, and H. Kronmüller, Rep. Prog. Phys. **65**, 651 (2002).

[26] C. P. Bean, Phys. Rev. Lett. **8**, 250 (1962); Rev. Mod. Phys. **36**, 31 (1964); J. Appl. Phys. **41**, 2482 (1970).

[27] E. H. Brandt, Low Temp. Phys. **27**, 723 (2001).

[28] C. Romero-Salazar and F. Pérez-Rodríguez, J. Non-Cryst. Solids **329**, 159 (2003); Supercond. Sci. Technol. **16**, 1273 (2003); Appl. Phys. Lett. **83**, 5256 (2003).

[29] F. Pérez-Rodríguez, A. Pérez-González, John R. Clem, G. Gandolfini, and M. A. R. LeBlanc, Phys. Rev. B **56**, 3473 (1997).

[30] C. Romero-Salazar, O. A. Hernández-Flores, and Ch. Jooss (unpublished).

[31] J. R. Cave and M. A. R. LeBlanc, J. Appl. Phys. **53**, 1631 (1948).

[32] A. Pérez-González and J. R. Clem, J. Appl. Phys. **58**, 4326 (1985).

[33] N. A. Frederick, S. Li, M. B. Maple, V. F. Nesterenko, and S. S. Indrakanti, Physica C **363**, 1 (2001); S. S. Indrakanti, V. F. Nesterenko, M. B. Maple, N. A. Frederick, W. H. Yuhasz, and Shi Li, Philos. Mag. Lett. **81**, 849 (2001).